Electronic Supplementary Material (ESI) for Journal of Materials Chemistry C.
This journal is © The Royal Society of Chemistry 2021

Supporting Information

β-$BaGa_4Se_7$: A Promising IR Nonlinear Optical Crystal Designed by Predictable Structural Rearrangement

Zhen Qian,[a] Qiang Bian,[b] Hongping Wu,[a] Hongwei Yu,*[a] Zheshuai, Lin,*[c] Zhanggui Hu,[a] Jiyang Wang,[a] and Yicheng Wu[a]

[a] *Tianjin Key Laboratory of Functional Crystal Materials, Institute of Functional Crystal, Tianjin University of Technology, Tianjin 300384, China.*

[b] *School of Material and Energy, Guangdong University of Technology, Guang Zhou, 510006, China.*

[c] *Beijing Center of Crystal R&D, Key Lab of Functional Crystals and Laser Technology, Chinese Academy of Sciences, Beijing, 100190, China.*

To whom correspondence should be addressed: hwyu15@gmail.com

CONTENTS

Experimental Procedures

Materials. Barium fluoride (Ba, 99%, Aladdin), Gallium selenide (Ga_2Se_3, 99.99%, Aladdin), Selenium (Se, 99.99%, Aladdin), all the reagents were commercially purchased without further refinement.

Syntheses. A mixture of Ba (0.364 mmol, 0.05 g), Ga_2Se_3 (0.93 mmol, 0.35 g), and Se (1.266 mmol, 0.1 g) was firstly loaded into a graphite crucible that avoids the reaction between alkaline earth metal (Ba) and silica tube, then put it into the silica tube and flame-sealed under 10^{-3} Pa. The tube was heated to 850 °C in 30 h and kept at this temperature for about 90 h, then slowly down to ambient temperature by 5 days. N, N−dimethylformamide (DMF) solvent was chosen to wash the products. Finally, many millimeter-level crystals for β-$BaGa_4Se_7$ (yellow) were found and stable in the air after several months.

Structural Refinement and Crystal Data. The data for β-$BaGa_4Se_7$ were collected from a shock-cooled single crystal at 100(2) K on a Bruker D8 VENTURE CCD diffractometer using the Mo Kα source (λ = 0.71073 Å) with the aid of the Bruker APEX II program. All data were integrated with SAINT and a numerical absorption correction using SADABS was applied.[1,2] The structure was solved by direct methods using SHELXT and refined by full-matrix least-squares methods against F^2 by SHELXL-2018/3.[3,4] Crystallographic data for the structures reported in this paper have been deposited with the Cambridge Crystallographic Data Centre.[5] CCDC 2048470 contain the supplementary crystallographic data for this paper. These data can be obtained free of charge from The Cambridge Crystallographic Data Centre via www.ccdc.cam.ac.uk/structures. Crystal data, data collection and structure refinement are summarized in Table S1. In Table S2, the final refined atomic coordinates, equivalent isotropic displacement parameters and the calculated bond valence sums (BVSs) of the title compound are collected. Selected bond distances are given in Table S3.

Powder X-ray Diffraction. The powder X-ray diffraction (PXRD) analysis was performed on a SmartLab 9KW X-ray diffractometer at room temperature (Cu-Kα radiation). The collected data is within the 2θ range of 10-70°, with a step size of 0.01° and a step time of 2 s.

UV−Vis−Near-IR (NIR) Diffuse-Reflectance and IR spectra. The UV/Vis/NIR diffuse reflectance spectrum was measured with a Shimadzu SolidSpec-3700DUV UV/Vis/NIR Spectrophotometer at room temperature. The measurement range from 300 to 2000 nm and the barium sulfate is used as the diffuse reflection standard. The IR spectra of β-$BaGa_4Se_7$ were recorded on a Nicolet iS50 Fourier transform infrared in the range 400-4000 cm^{-1}. A sample of ~10 mg was used for testing.

Raman Spectroscopy. Raman spectra on the crushed crystals of title compounds were collected by a LABRAM HR Evolution spectrometer equipped with a CCD detector using 532 nm radiation from a diode laser. For each sample, crystals were

placed on a glass slide and a 50 × objective lens was used to choose the area of the crystal specimens to be measured. The grating was set to be 600 gr per mm. The maximum power of 60 mW and beam diameter of 35 μm was used. The spectrum was collected using an integration time of 5 s.

Power SHG Measurement. The SHG response for the title compound was measured according to the method proposed by Kurtz and Perry with laser radiation at an optical wavelength of 1064 nm. Powder samples of β-$BaGa_4Se_7$ crystals were graded into several distinct particle size ranges of 25–53, 53–75, 75–106, 106–120, 120–150, 150–180 and 180–212 μm. At the same time, a powder AGS sample with the same particle size range was used as a reference.

Birefringence Measurement. The birefringence of β-$BaGa_4Se_7$ was measured by using a cross-polarizing microscope. On the basis of the crystal optics, following the equation $R = \Delta n \times d$, Δn can be obtained, where R, Δn, and d are retardation, birefringence, and thickness, respectively. For the birefringent measurements, a triangle β-$BaGa_4Se_7$ crystal with a thickness of 7.8 μm was used (Figure 4c).

The details of computational methods. The total energy calculations, phonon frequencies, electronic structure and optical properties were calculated by Perdew−Burke−Ernzerhof (PBE) generalized gradient approximation functional with norm-conserving pseudopotentials,[6] as implanted in the CASTEP plane-wave code.[7] The PAW potentials used the $5s^25p^66s^2$, $3d^{10}4s^24p^1$, and $4s^24p^4$ as valence electrons of the Ba, Ga and Se atoms, respectively. An energy cutoff of 860 eV and dense Monkhorst-Pack k-mesh of 0.18 $Å^{-1}$ were adopted to achieve good convergence for the first principle calculations. The optical property calculations were scissor-corrected (0.972 eV) by the energy gap difference between the PBE and the experimental values. SHG calculations have previously been used to analyze borate NLO crystals.[8]

Table S1. Crystal data and structure refinement for *β*-$BaGa_4Se_7$.

CCDC number	2048470
Empirical formula	$BaGa_4Se_7$
Formula weight	968.94
Temperature [K]	100(2)
Crystal system	orthorhombic
Space group (number)	$Pna2_1$ (No. 33)
a [Å]	15.4385(12)
b [Å]	7.6109(6)
c [Å]	10.5210(7)
Volume [$Å^3$]	1236.23(16)
Z	4
Density [g/cm^3]	5.206
μ [mm^{-1}]	32.298
$F(000)$	1672
Crystal size [mm^3]	0.064×0.066×0.067
Crystal color	yellow
Crystal shape	block
Radiation	MoK_α (λ=0.71073 Å)
2θ range [°]	5.28 to 54.98 (0.77 Å)
Index ranges	$-20 \le h \le 19$ $-7 \le k \le 9$ $-13 \le l \le 13$
Reflections collected	7486
Independent reflections	2772, R_{int} = 0.0376, R_{sigma} = 0.0455
Completeness to θ = 25.242°	99.9 %
Data / Restraints / Parameters	2772/1/110
Goodness-of-fit on F^2	1.027
Final R indices [$F_o^2 > 2s(F_o^2)$][a]	R_1 = 0.0358, wR_2 = 0.0659
Final R indexes [all data]	R_1 = 0.0463, wR_2 = 0.0716
Largest peak/hole [e·$Å^{-3}$]	1.31/-2.08

[a] $R_1 = \Sigma||F_o| - |F_c||/\Sigma|F_o|$ and $wR_2 = [\Sigma w(F_o^2 - F_c^2)^2 / \Sigma w F_o^4]^{1/2}$ for $F_o^2 > 2\sigma(F_o^2)$

Table S2. Atomic coordinates, U_{eq} [Å^2] and bond valence sums (BVS) for *β*-$BaGa_4Se_7$.

Atom	*x*	*y*	*z*	U_{eq}	BVS
Ba1	0.37646(7)	-0.00476(11)	0.74351(9)	0.0139(2)	1.73
Ga1	0.37411(9)	0.7491(2)	0.39201(16)	0.0049(3)	3.12
Ga2	0.25939(10)	0.4900(2)	0.61939(17)	0.0055(4)	3.07
Ga3	0.37049(10)	0.2542(2)	0.37620(16)	0.0054(4)	3.13
Ga4	0.49430(11)	0.4839(2)	0.61445(16)	0.0059(3)	3.04
Se1	0.49870(9)	0.2174(2)	0.49459(13)	0.0063(4)	1.97
Se2	0.23428(9)	0.2517(2)	0.47733(15)	0.0088(3)	1.94
Se3	0.37736(10)	0.45300(19)	0.76193(14)	0.0098(3)	1.91
Se4	0.24695(9)	0.76615(19)	0.51522(15)	0.0087(3)	1.94
Se5	0.36784(11)	0.51129(17)	0.23750(14)	0.0049(3)	2.21
Se6	0.50056(9)	0.7672(3)	0.51804(15)	0.0063(3)	1.94
Se7	0.37928(11)	0.99372(16)	0.24211(14)	0.0045(3)	2.18

U_{eq} is defined as 1/3 of the trace of the orthogonalized U_{ij} tensor.

Table S3. Bond lengths and angles for *β*-$BaGa_4Se_7$.

Atom–Atom	**Length [Å]**	$Se4^{\#1}$–Ba1–$Se1^{\#3}$	124.40(4)
Ba1–Se3	3.4893(17)	Se1–Ba1–$Se1^{\#3}$	116.91(3)
Ba1–$Se6^{\#1}$	3.509(2)	Se3–Ba1–$Se7^{\#4}$	88.51(3)
Ba1–$Se2^{\#2}$	3.523(2)	$Se6^{\#1}$–Ba1–$Se7^{\#4}$	57.48(3)
Ba1–$Se4^{\#1}$	3.5786(19)	$Se2^{\#2}$–Ba1–$Se7^{\#4}$	119.98(4)
Ba1–Se1	3.6440(19)	$Se4^{\#1}$–Ba1–$Se7^{\#4}$	124.53(4)
Ba1–$Se1^{\#3}$	3.6484(19)	Se1–Ba1–$Se7^{\#4}$	57.93(3)
Ba1–$Se7^{\#4}$	3.7718(16)	$Se1^{\#3}$–Ba1–$Se7^{\#4}$	58.98(3)
Ba1–$Se5^{\#2}$	3.7742(18)	Se3–Ba1–$Se5^{\#2}$	88.43(4)
Ga1–Se4	2.356(2)	$Se6^{\#1}$–Ba1–$Se5^{\#2}$	123.39(4)
Ga1–Se6	2.364(2)	$Se2^{\#2}$–Ba1–$Se5^{\#2}$	62.85(4)
Ga1–Se5	2.435(2)	$Se4^{\#1}$–Ba1–$Se5^{\#2}$	56.37(3)
Ga1–Se7	2.441(2)	Se1–Ba1–$Se5^{\#2}$	119.37(4)
Ga2–Se3	2.376(2)	$Se1^{\#3}$–Ba1–$Se5^{\#2}$	123.67(4)
Ga2–Se4	2.378(2)	$Se7^{\#4}$–Ba1–$Se5^{\#2}$	176.65(4)
Ga2–Se2	2.382(2)	Se4–Ga1–Se6	112.10(10)
Ga2–$Se7^{\#2}$	2.500(2)	Se4–Ga1–Se5	112.03(9)
Ga3–Se1	2.356(2)	Se6–Ga1–Se5	116.79(9)
Ga3–Se2	2.357(2)	Se4–Ga1–Se7	109.92(9)
Ga3–$Se7^{\#1}$	2.437(2)	Se6–Ga1–Se7	106.91(9)
Ga3–Se5	2.441(2)	Se5–Ga1–Se7	97.87(7)
Ga4–Se6	2.385(3)	Se3–Ga2–Se4	117.23(8)
Ga4–Se1	2.389(2)	Se3–Ga2–Se2	115.50(8)
Ga4–Se3	2.392(2)	Se4–Ga2–Se2	111.75(10)
Ga4–$Se5^{\#4}$	2.492(2)	Se3–Ga2–$Se7^{\#2}$	109.38(9)
Atom–Atom–Atom	**Angle [°]**	Se4–Ga2–$Se7^{\#2}$	99.14(7)
Se3–Ba1–$Se6^{\#1}$	121.96(5)	Se2–Ga2–$Se7^{\#2}$	101.15(7)
Se3–Ba1–$Se2^{\#2}$	119.24(5)	Se1–Ga3–Se2	120.67(10)
$Se6^{\#1}$–Ba1–$Se2^{\#2}$	118.49(5)	Se1–Ga3–$Se7^{\#1}$	99.35(8)
Se3–Ba1–$Se4^{\#1}$	121.73(4)	Se2–Ga3–$Se7^{\#1}$	107.73(9)
$Se6^{\#1}$–Ba1–$Se4^{\#1}$	67.07(4)	Se1–Ga3–Se5	115.19(9)
$Se2^{\#2}$–Ba1–$Se4^{\#1}$	86.63(4)	Se2–Ga3–Se5	105.15(9)
Se3–Ba1–Se1	64.83(4)	$Se7^{\#1}$–Ga3–Se5	107.87(7)
$Se6^{\#1}$–Ba1–Se1	57.37(4)	Se6–Ga4–Se1	122.82(9)
$Se2^{\#2}$–Ba1–Se1	175.81(5)	Se6–Ga4–Se3	113.28(8)
$Se4^{\#1}$–Ba1–Se1	91.90(4)	Se1–Ga4–Se3	106.29(8)
Se3–Ba1–$Se1^{\#3}$	113.61(4)	Se6–Ga4–$Se5^{\#4}$	99.96(7)
$Se6^{\#1}$–Ba1–$Se1^{\#3}$	88.95(4)	Se1–Ga4–$Se5^{\#4}$	105.22(8)
$Se2^{\#2}$–Ba1–$Se1^{\#3}$	61.15(4)	Se3–Ga4–$Se5^{\#4}$	108.01(9)

Symmetry transformations used to generate equivalent atoms:
#1: +X, -1+Y, +Z; #2: 0.5-X, -0.5+Y, 0.5+Z; #3: 1-X, -Y, 0.5+Z; #4: 1-X, 1-Y, 0.5+Z.

Table S4a. The dipole moments of $[GaSe_4]^{5-}$ and $[BaSe_8]^{14-}$ groups in α-$BaGa_4Se_7$.

Polyhedron	X-axis Dipole moment	Y-axis Dipole moment	Z-axis Dipole moment	magnitude
$[Ga(1)Se_4]^{5-}$	-0.57	0	6.51	6.82
$[Ga(2)Se_4]^{5-}$	-7.76	0	-14.71	12.58
$[Ga(3)Se_4]^{5-}$	9.62	0	5.41	8.24
$[Ga(4)Se_4]^{5-}$	6.70	0	12.62	10.79
$[BaSe_8]^{14-}$	9.91	0	2.68	8.82
Unit cell	17.9	0	12.51	15.64

Table S4b. The dipole moments of $[GaSe_4]^{5-}$ and $[BaSe_8]^{14-}$ groups in β-$BaGa_4Se_7$.

Polyhedron	X-axis Dipole moment	Y-axis Dipole moment	Z-axis Dipole moment	magnitude
$[Ga(1)Se_4]^{5-}$	0	0	-17.73	17.73
$[Ga(2)Se_4]^{5-}$	0	0	5.02	5.02
$[Ga(3)Se_4]^{5-}$	0	0	-17.27	17.27
$[Ga(4)Se_4]^{5-}$	0	0	27.95	27.95
$[BaSe_8]^{14-}$	0	0	-43.04	43.04
Unit cell	0	0	-45.07	45.07

Table S5. The space groups, $GaSe_4$ tetrahedral number, flexibility indices (*F*), SHG responses (×AGS) and birefringence (Δ*n*) of $AgGaSe_2$ and *β*-$BaGa_4Se_7$.

Crystal	Space groups	Anion groups	tetrahedral number/unit	*F*	SHG	Δ*n*
$AgGaSe_2$	*I*-42*d*/nonpolar	$GaSe_4$	10	0.161	3	0.02
β-$BaGa_4Se_7$	$Pna2_1$/polar	$GaSe_4$	18	0.174	5	0.04

For nonpolar compounds, it seems to be difficult to understand the origin of SHG response from the dipole moments of the anion groups. However, the SHG responses of materials are related to not only the intrinsic dipole moments but also the induced dipole moments, which have been considered to have a more significant effect. The flexibility index was proposed to characterize the induced polarizability by valence electrons.[9] In 2014, Jiang *et al*. proposed a simple "flexible dipole model" to 'quantify' the induced dipole moments by calculating an empirical "flexibility index" *F* based on the following equation: [10]

$$F = \frac{\exp\left[\left(R_0 - R_a\right)/B\right]}{\left(\sqrt{C_a} + \sqrt{C_b}\right)^2 / {R_a}^2}$$

where R_a is the average bond length of the group, R_0 is the tabulated ideal bond length, *B* is an empirical constant, typically 0.37 Å, and C_a (C_b) is the outermost electron of an atom. We can know that C_a and C_b for Ga and Se are 5 and 8, respectively.

Clearly, the flexibility index calculations reveal that $GaSe_4$ tetrahedra in *β*-$BaGa_4Se_7$ are more "flexible" than the $AgGaSe_2$, indicating that the former groups are easier to generate the larger induced polarization compared with the latter, combined with the higher number of the $GaSe_4$ tetrahedra in the unit cell (*β*-$BaGa_4Se_7$:18 *vs.* $AgGaSe_2$:10), that makes the SHG response and birefringence significantly enhanced from $AgGaSe_2$ (SHG = 3 × AGS, Δ*n* = 0.02) to *β*-$BaGa_4Se_7$ (SHG = 5 × AGS, Δ*n* = 0.04).

Figure S1. Phonon dispersions of β-$BaGa_4Se_7$ at ambient pressure. The absence of any imaginary frequency in the whole Brillouin zone demonstrates that β-$BaGa_4Se_7$ is dynamically stable.

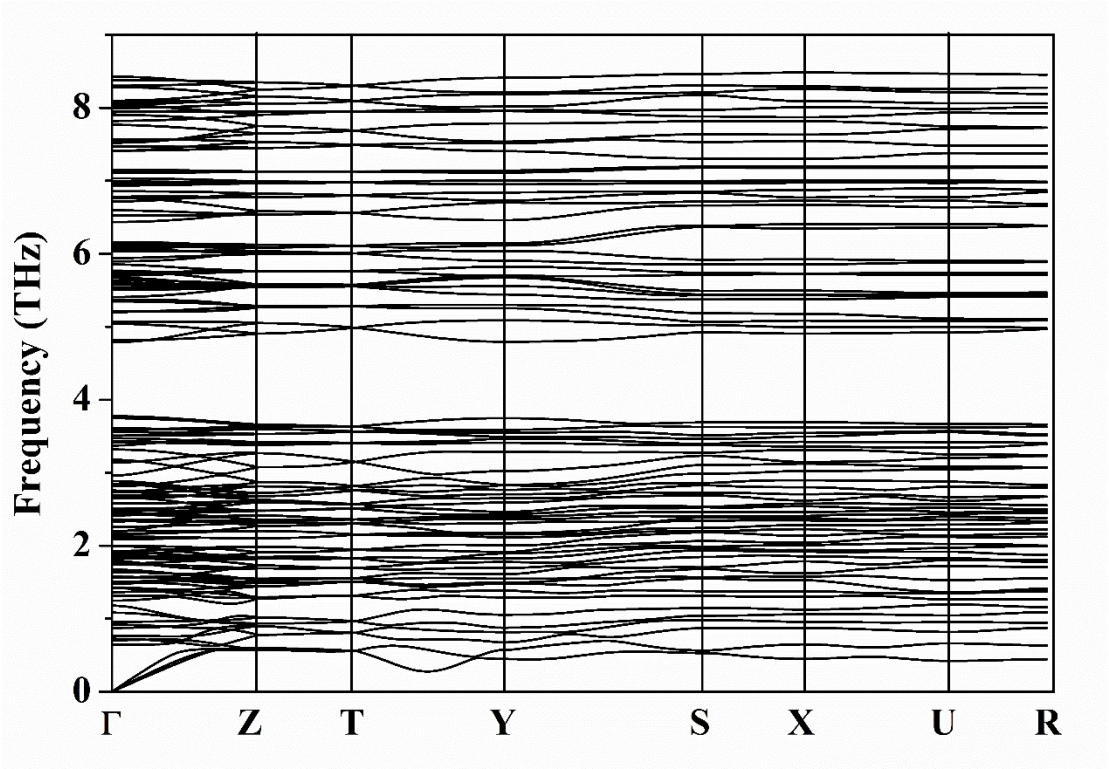

Figure S2. The Powder XRD patterns of *β*-$BaGa_4Se_7$. The polycrystalline XRD pattern of the title compound is in good agreement with the calculated.

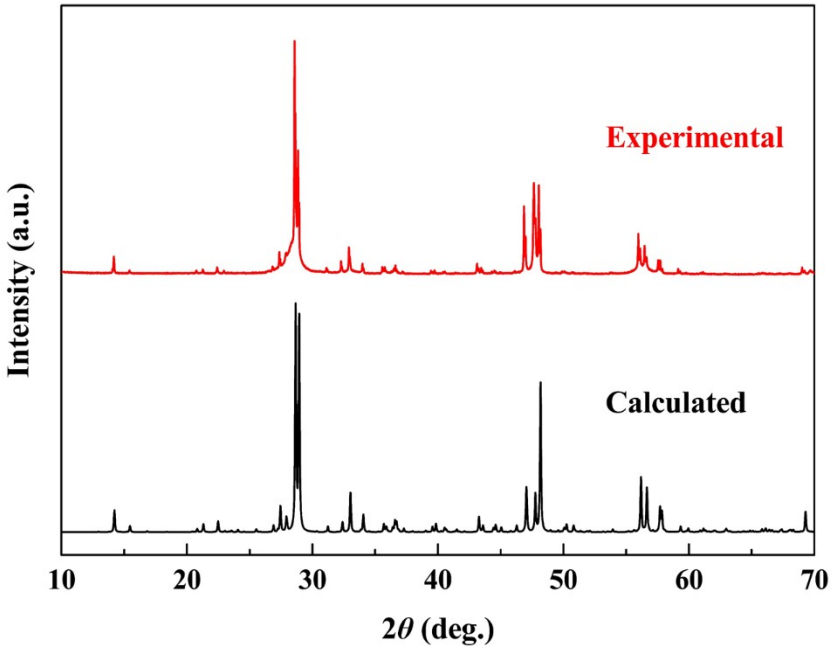

Figure S3. The variable-temperature powder XRD patterns of the *β*-$BaGa_4Se_7$. The variable-temperature powder XRD measurement confirms that *β*-$BaGa_4Se_7$ is stable from room temperature to 900 °C. After 900 °C, *β*-$BaGa_4Se_7$ starts to transfer to the *α*- $BaGa_4Se_7$.

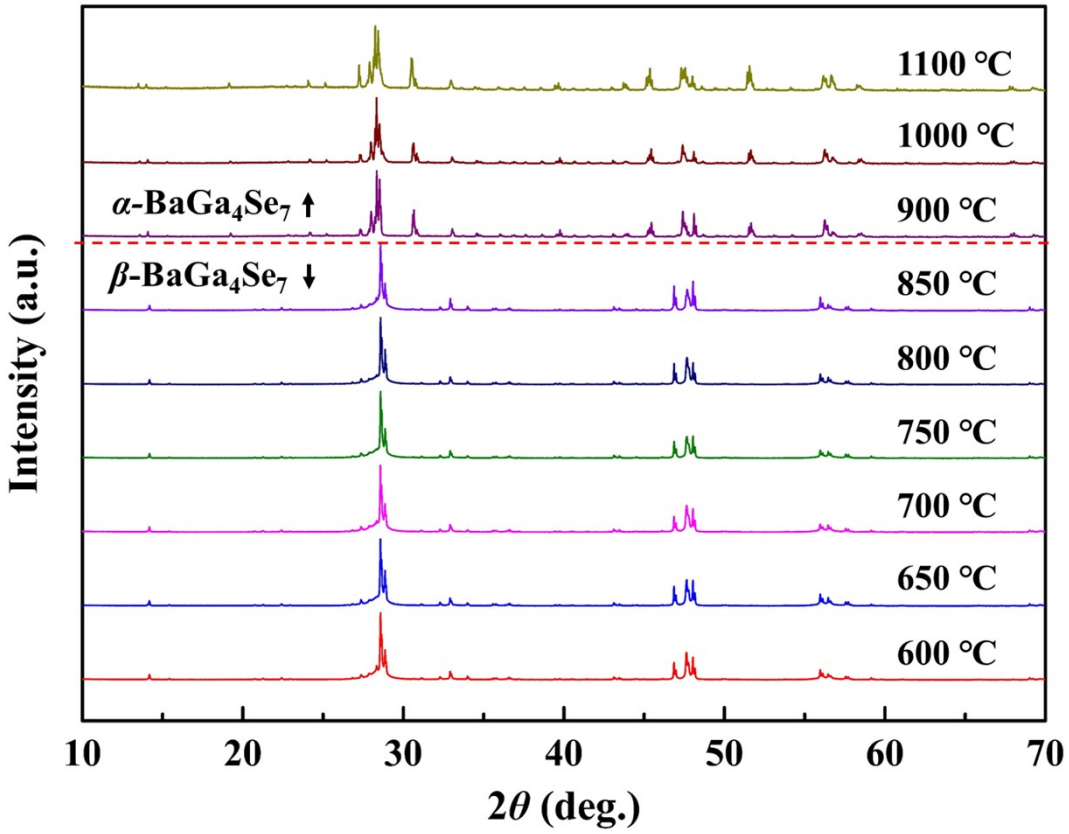

Figure S4. The powder XRD patterns of the α-$BaGa_4Se_7$ after 850 ℃ for 72h. When α-$BaGa_4Se_7$ was calcined at 850 °C for 72 h, no phase-transition from α-$BaGa_4Se_7$ to β-$BaGa_4Se_7$ was observed. That indicates the phase-transition from β-$BaGa_4Se_7$ to α-$BaGa_4Se_7$ is irreversible.

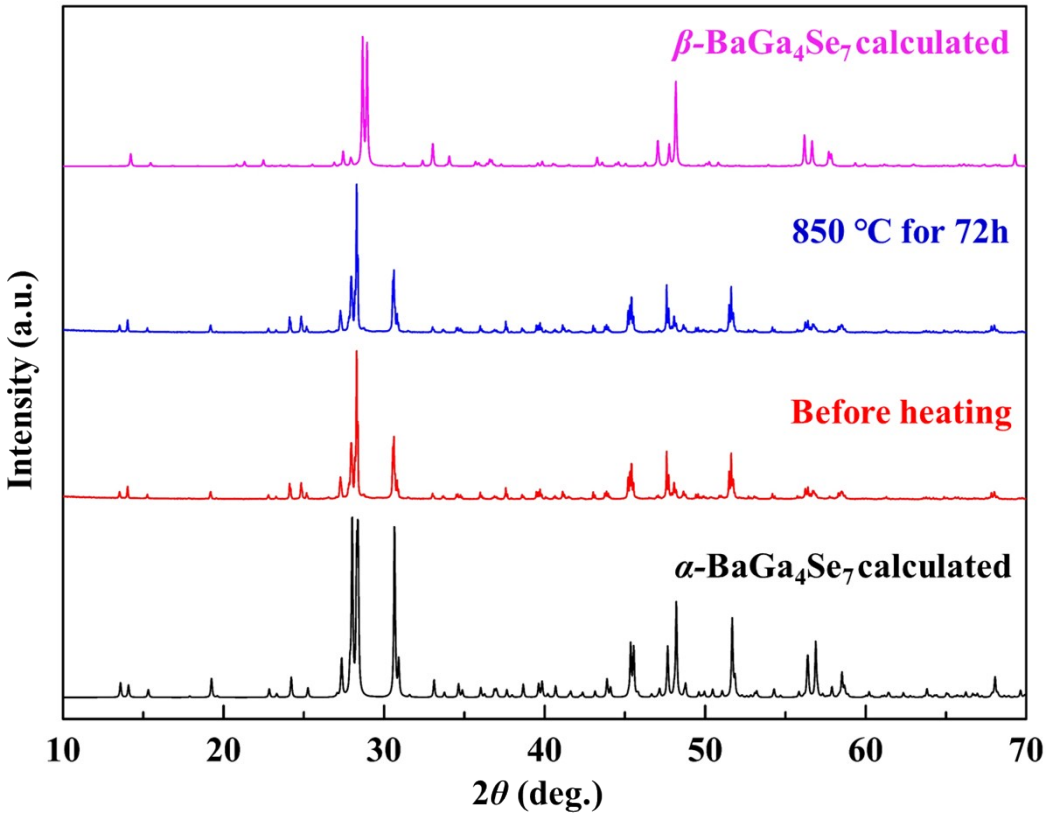

Figure S5. The UV-Vis-NIR diffuse reflectance spectra for *β*-$BaGa_4Se_7$. The cut-off edge of *β*-$BaGa_4Se_7$ is about 440 nm. Correspondingly, its band-gap can be calculated as 2.82 eV.

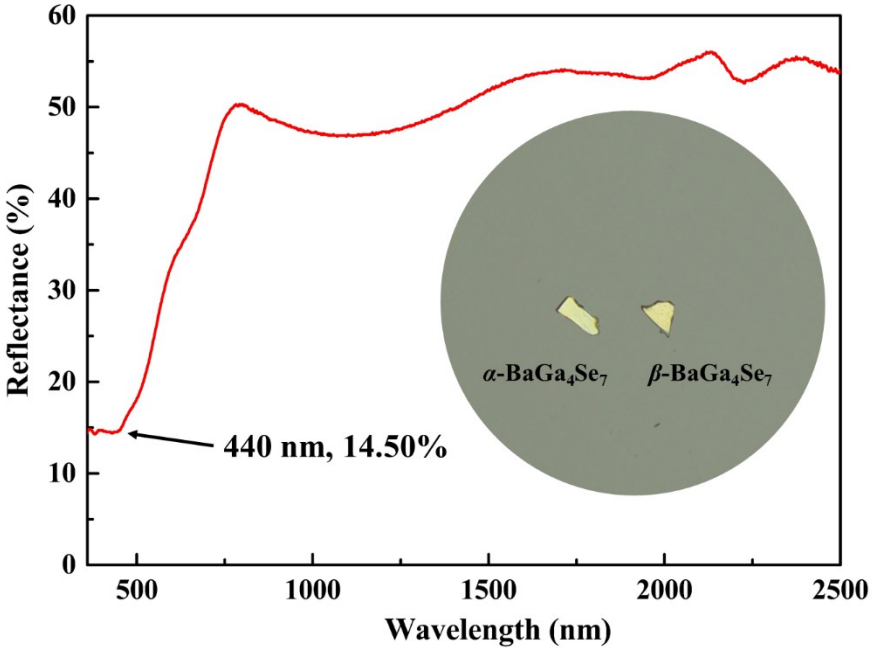

Figure S6. IR spectra for *β*-$BaGa_4Se_7$. It has no obvious absorption in a wide range from 4000 to 500 cm^{-1} (*i.e.* 2.5~20 μm), implying that *β*-$BaGa_4Se_7$ may have a wide IR transmission region and cover two important atmospheric windows, 3-5 and 8-14 μm.

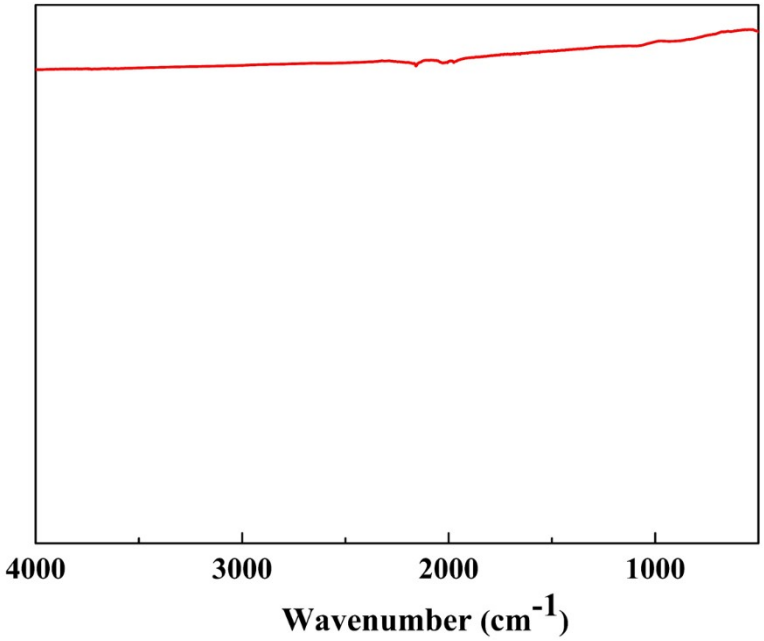

Figure S7. Raman spectra of *β*-$BaGa_4Se_7$. The absorption between the 180-240 cm^{-1} can be assigned to the characteristic vibration of the Ga-Se mode, and other Raman peaks below 180 cm^{-1} are due to the Ba-Se vibrations.

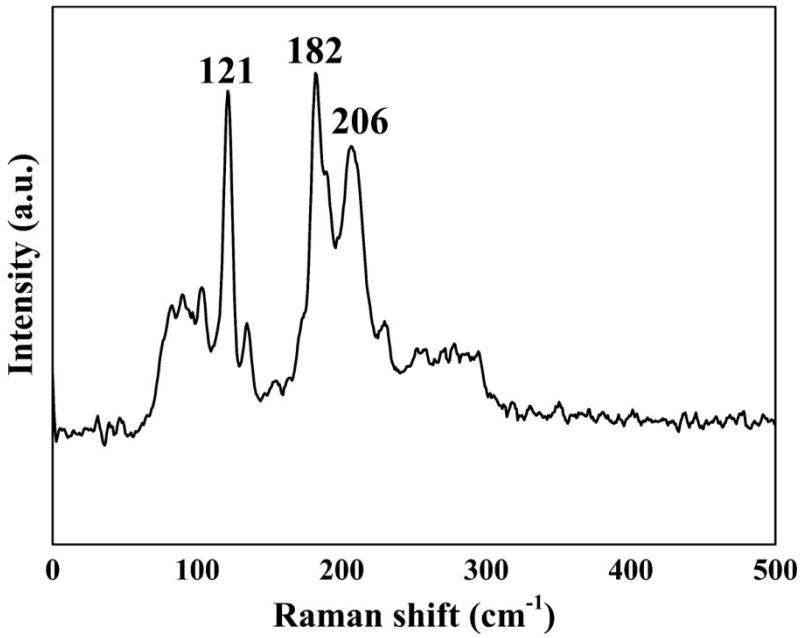

Figure S8. Crystal for the birefringence determination and the interference colors observed in the cross-polarized light for *β*-$BaGa_4Se_7$. The birefringence in the visible region can be calculated as 0.040 for *β*-$BaGa_4Se_7$.

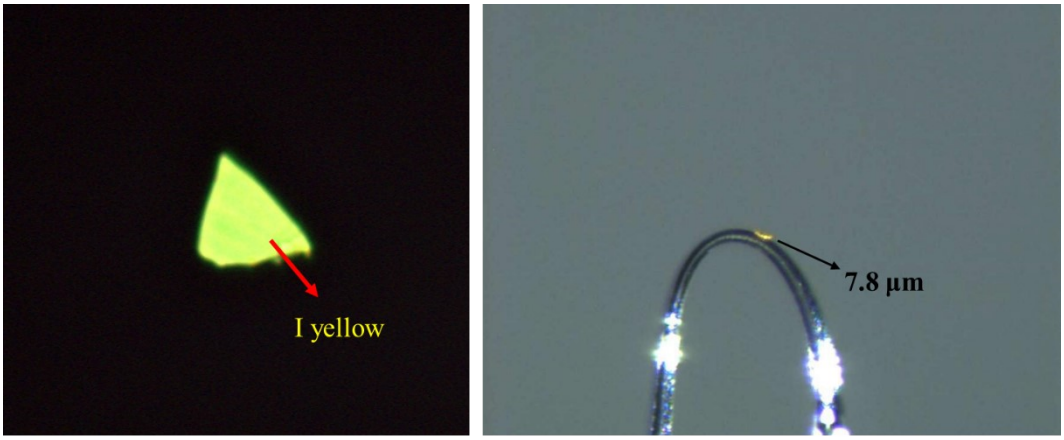

(a) (b)

Figure S9. The calculated refractive index and birefringence based on the first principles. The calculated birefringence of β-$BaGa_4Se_7$ is in the range of 0.057-0.031 from 500 to 2000 nm, which are similar to measured values.

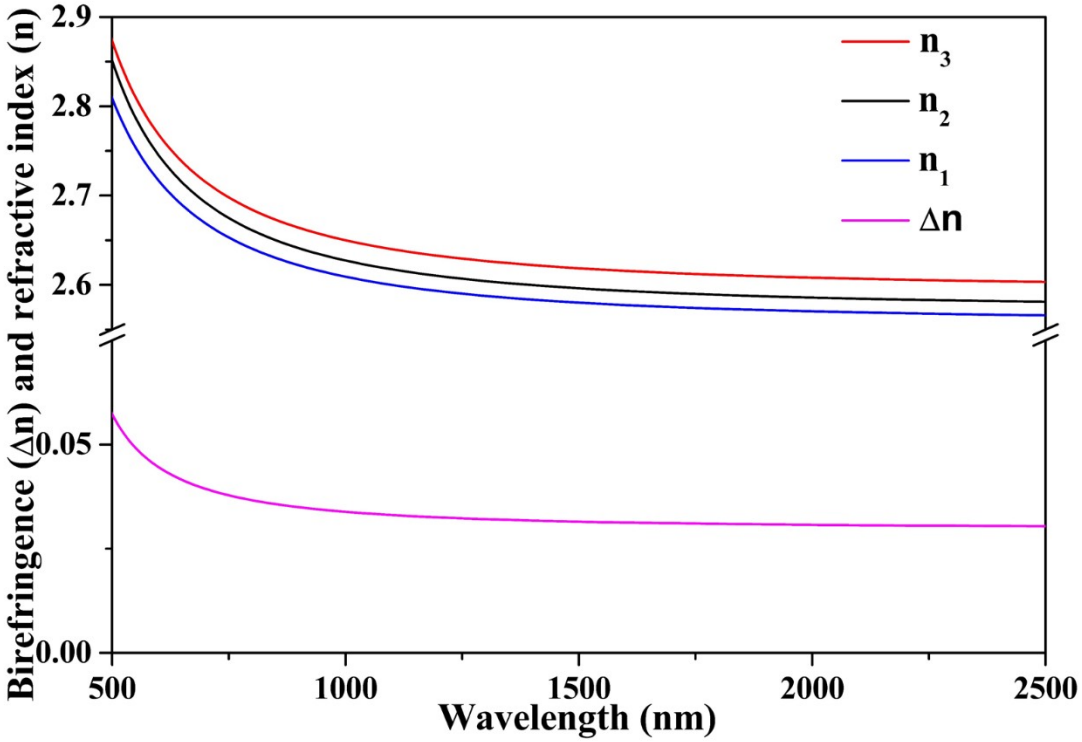

Figure S10. The calculated phase matching based on the first principles. The results show that β-$BaGa_4Se_7$ is able to achieve phase matching in the whole Mid-IR wavelengths and cover two important atmospheric windows, 3~5 μm and 8~12 μm.

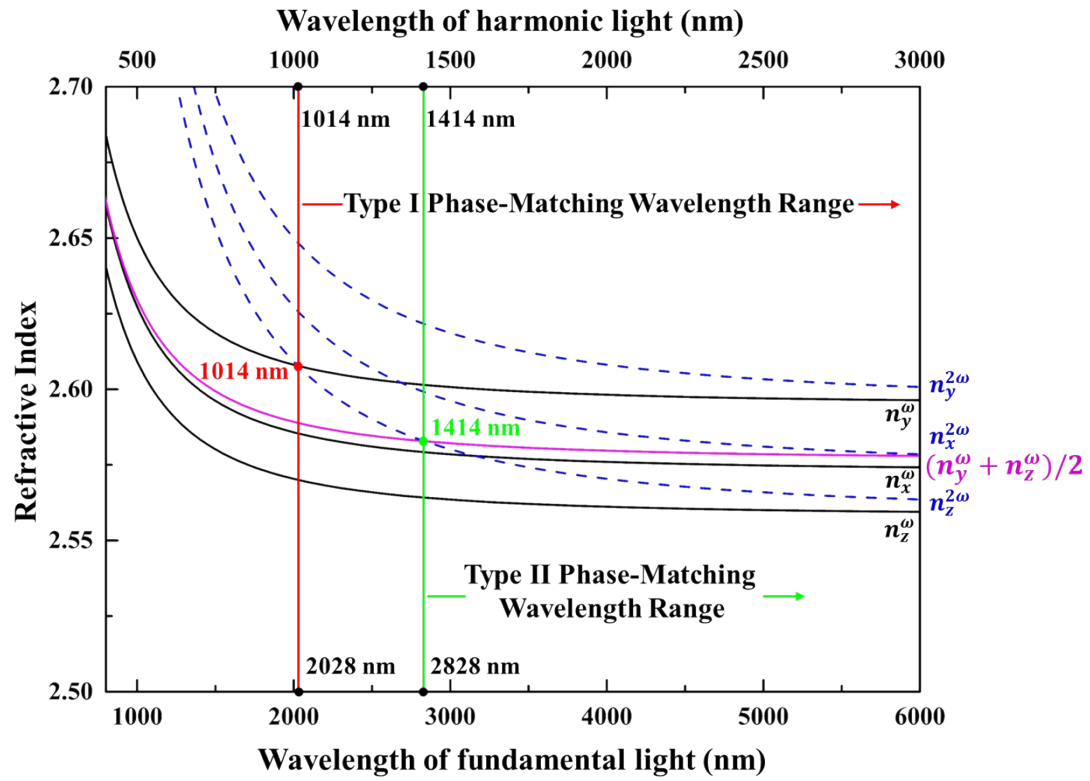

Figure S11. The Ga-Se bond lengths, polarization directions and dipole moments of [$GaSe_4$] polyhedra in α- and β-$BaGa_4Se_7$. The direction indicated by the red arrow is the polarization direction of the [GaSe4] polyhedra.

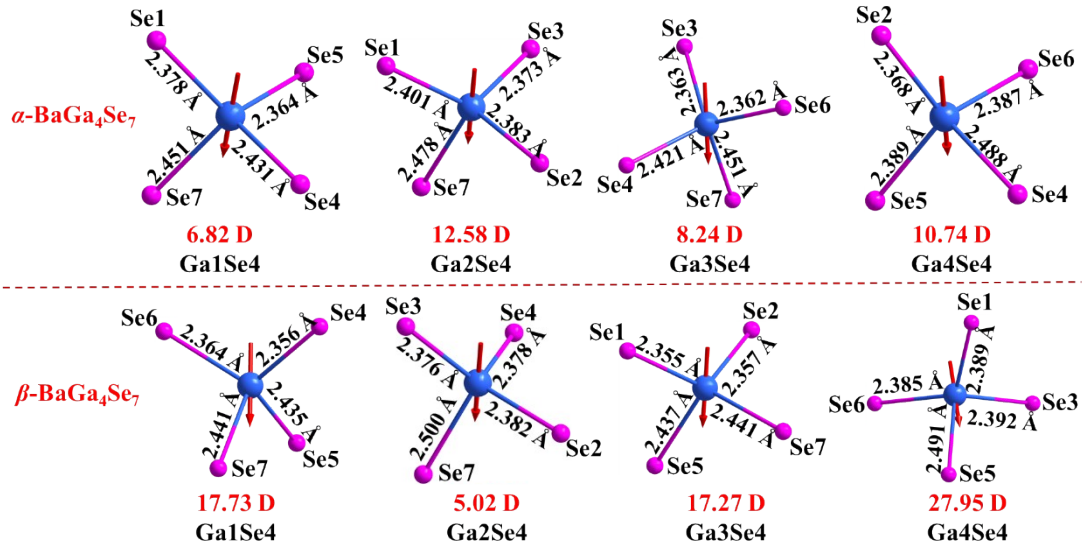

Figure S12. The SHG signals for α- and β-$BaGa_4Se_7$ in the same particle sizes. The SHG signal of β-$BaGa_4Se_7$ is stronger (~1.5 times) than that of α-$BaGa_4Se_7$ at the same condition.

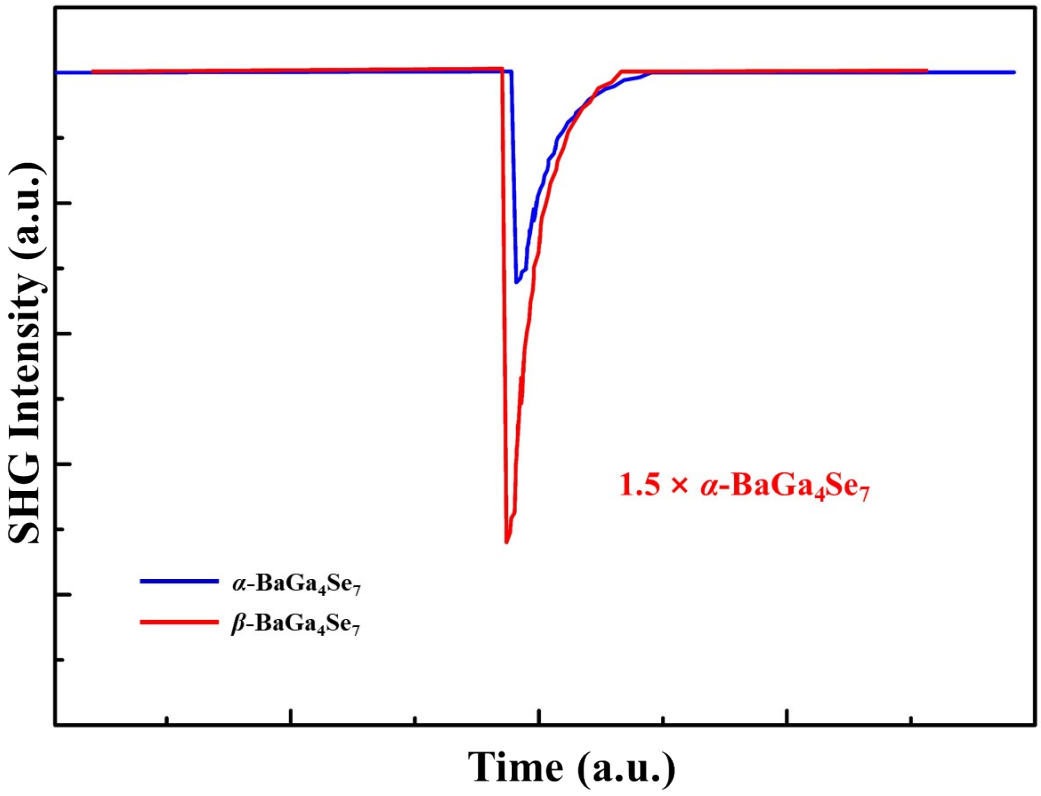

Figure S13. The topological structure of $AgGaSe_2$ and β-$BaGa_4Se_7$. (a) The topological structure of $AgGaSe_2$ with the $[GaSe_4]$ units regarded as the nodes; (b) The Topological structure of β-$BaGa_4Se_7$ with the $[Ga_4Se_{10}]$ units regarded as the nodes.

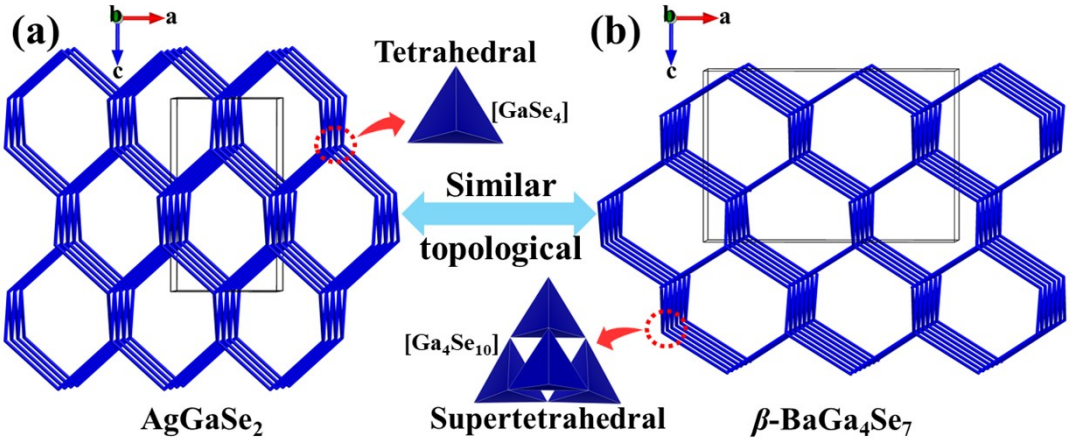

Figure S14. Band structure of *β*-$BaGa_4Se_7$ calculated by PBE functional. *β*-$BaGa_4Se_7$ has a direct band gap of 1.85 eV, which is smaller than that of experimental value (2.82 eV) owing to the discontinuity of exchange-correlation energy.

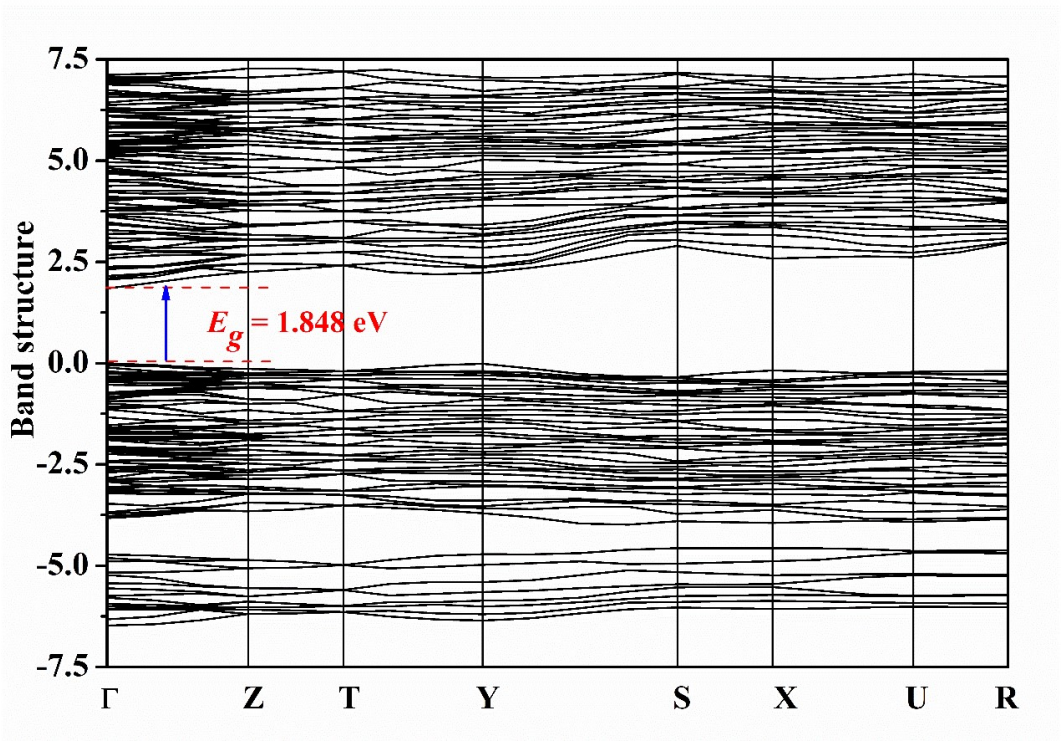

Figure S15. The density of states of β-$BaGa_4Se_7$ structure. The partial density of states analysis of transitions from occupied states to unoccupied states reveals the microcosmic origin of the optical properties from an electronic level insight. The 4s, 4p states of Ga and 4s, 4p states of Se construct the top region of valence states from -7.5 to 0 eV. Their wide hybridization in this area indicates that Ga-Se bonds make the main contribution of the upper side of the valence band. The bottom region of conduction states mainly is composed of 4s, 4p states of Ga, 4s, 4p states of Se and 4d, 6s states of Ba. Thus, [$GaSe_4$] tetrahedra have a significant effect on its optical properties, thus, Ga-Se polyhedra composed of Ga-Se bonds determine the SHG effects of β-$BaGa_4Se_7$.

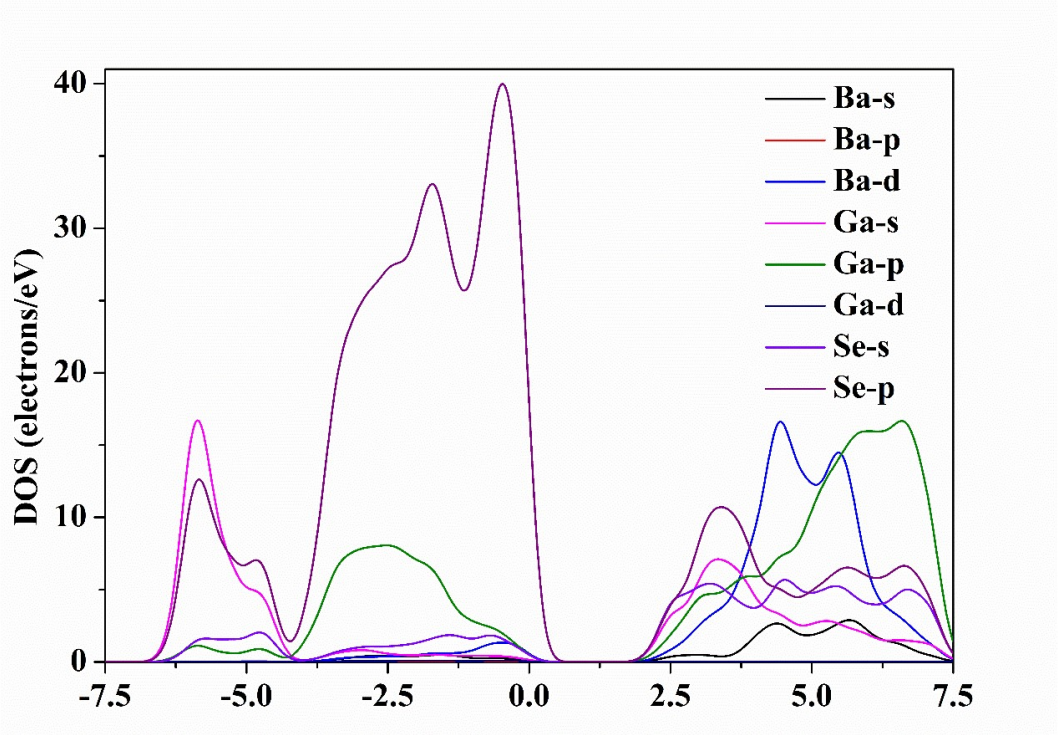

References

1. Bruker, SAINT, V8.40B, Bruker AXS Inc., Madison, Wisconsin, USA.
2. Bruker, SADABS, 2016/2, Bruker AXS Inc., Madison, Wisconsin, USA.
3. G. M. Sheldrick, *Acta Cryst.* 2015, **A71**, 3.
4. G. M. Sheldrick, *Acta Cryst.* 2015, **C71**, 3.
5. C. R. Groom, I. J. Bruno, M. P. Lightfoot, S. C. Ward, *Acta Cryst.* 2016, **B72**, 171.
6. J. Perdew, K. Burke, M. Ernzerhof, *Phys. Rev. Lett.* 1996, **77**, 3865.
7. S. J. Clark, M. D. Segall, C. J. Pickard, P. J. Hasnip, M. I. J. Probert, K. Refson, M. C. Payne, *Z. Kristallogr.* 2005, **220**, 567.
8. Y. Wang, S. L. Pan, *Coord. Chem. Rev.* 2016, **323**, 15.
9. B. F. Levin, *Phys. Rev. Lett.* 1969, **22**, 787.
10. X. X. Jiang, S. G. Zhao, Z. S. Lin, J. H. Luo, P. D. Bristowe, X. G. Guan, C. T. Chen *J. Mater. Chem. C*, 2014, **2**, 530.